b

UNIVERSITY
OF BERN

X-ray microtomography

485018-HS2025-0: Advanced Course II Ultraprecision Engineering

David Haberthür
Institute of Anatomy, September 16, 2025

Grüessech mitenang!

- David Haberthür
  - Physicist by trade
  - PhD in high resolution imaging of the lung, Institute of Anatomy, University of Bern, Switzerland
  - Post-Doc I: TOMCAT, Swiss Light Source, Paul Scherrer Institute, Switzerland
  - Post-Doc II: µCT group, Institute of Anatomy, University of Bern, Switzerland

Grüessech from the µCT group

David.Haberthuer@unibe.ch Ruslan.Hlushchuk@unibe.ch Oleksiy.Khoma@unibe.ch

µCT-group

- microangioCT [1]
  - Angiogenesis: heart, musculature [2] and bones
  - Vasculature: (mouse) brain [3], (human) nerve scaffolds [4], (human) skin flaps [5] and tumors
- Zebrafish musculature and gills [6]
- (Lung) tumor detection and metastasis classification [7]
- Collaborations with museums [8] and scientist at UniBe [9] to scan a wide range of specimens
- Automate *all* the things! [10, 11]

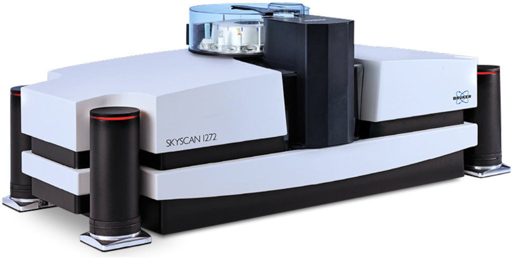

bruker.com/skyscan1272

Contents

Overview & Imaging methods

Tomography
- History
- Interaction of x-rays with matter
- Tomography today

A scan, from *getting started* to *nice image*

Examples
- A study about teeth
  - Overview
  - Materials & Methods
  - Results
- Metal foam analysis
- A study on fish

µCT

- Dense and/or non-transparent samples
- Calibrated & isotropic 3D images at micron resolutions
- Covers a very large range of sample sizes
- Gives information at different length scales
- Nondestructive imaging, thus compatible with routine sample preparation.
  Enables correlative imaging pipelines, scanning of museum & collection material

Biomedical imaging

- Medical research
- Non-destructive insights into the samples
- (Small) Biological samples

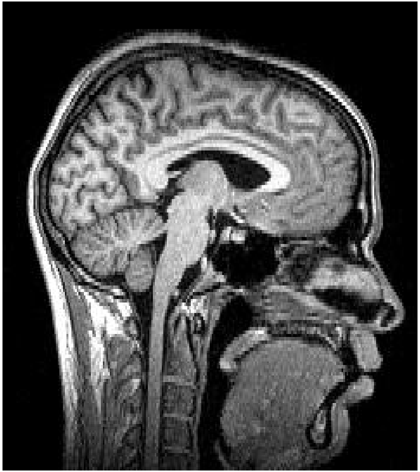

Biomedical imaging

- Medical resear
- Non-destruc
- (Small) Biol

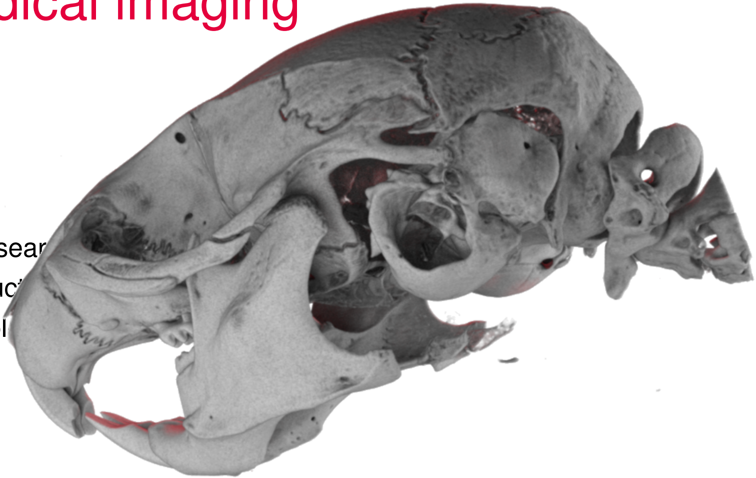

Wavelengths & Scales

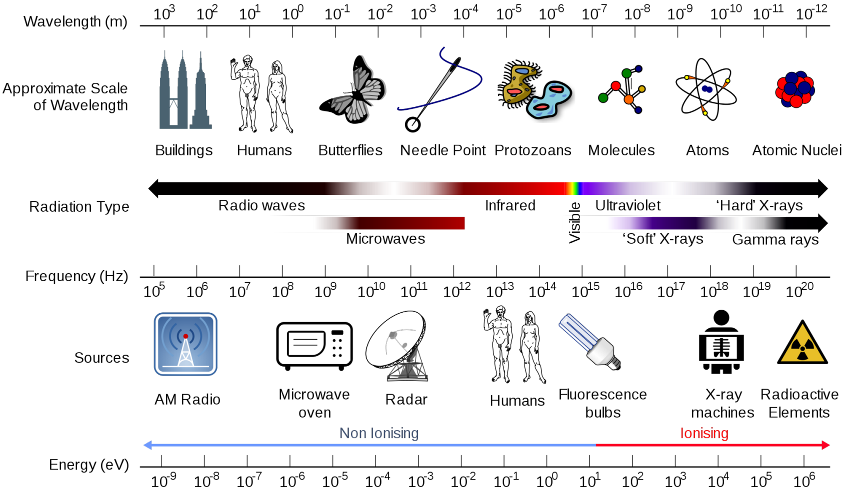

w.wiki/7fz

Wavelengths & Scales

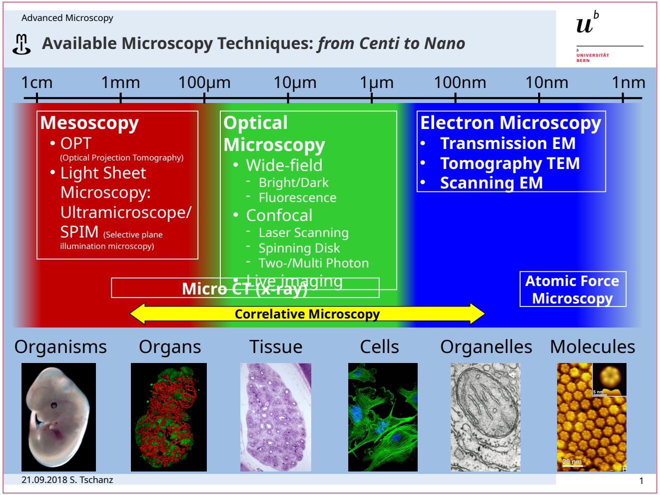

Introduction to Microscopy by Stefan Tschanz, Slide 1

Imaging methods

- Light (sheet) microscopy: see lecture of Nadia Mercader Huber
- X-ray imaging
- Electron microscopy
  - *Analytical electron microscopy* by Dimitri
  - *SEM Grundlagen* by Sabine Kässmeyer and Ivana Jaric
  - *Cryoelectron Microscopy & Serial Block Face SEM* by Ioan

CT-Scanner

youtu.be/2CWpZKuy-NE

CT History

- 1895: Wilhelm Conrad Röntgen discovers X-rays

w.wiki/BHAN

CT History

- 1895: Wilhelm Conrad Röntgen discovers X-rays
- 1963: Cormack used a collimated ^{60}Co source and a Geiger counter as a detector [12]
- 1976: Hounsfield worked on first clinical scanner [13]

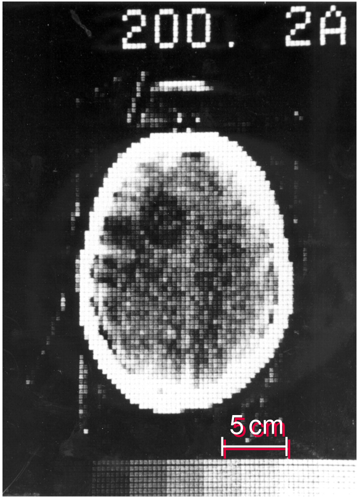

From [14], Figure 5

CT History

- 1895: Wilhelm Conrad Röntgen discovers X-rays
- 1963: Cormack used a collimated ^{60}Co source and a Geiger counter as a detector [12]
- 1976: Hounsfield worked on first clinical scanner [13]
- Nobel Prize in 1979, jointly for Allan Cormack and Godfrey Hounsfield

U.S. Patent Feb. 24, 1976 Sheet 1 of 2 3,940,625

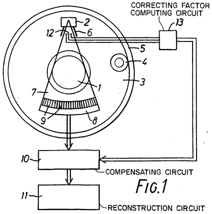

FIG.1

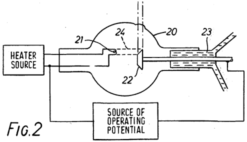

FIG.2

From [**US3940625A**], p. 2

CT History

- 1895: Wilhelm Conrad Röntgen discovers X-rays
- 1963: Cormack used a collimated ^{60}Co source and a Geiger counter as a detector [12]
- 1976: Hounsfield worked on first clinical scanner [13]
- Nobel Prize in 1979, jointly for Allan Cormack and Godfrey Hounsfield
- CT scanner generations
  - First generation

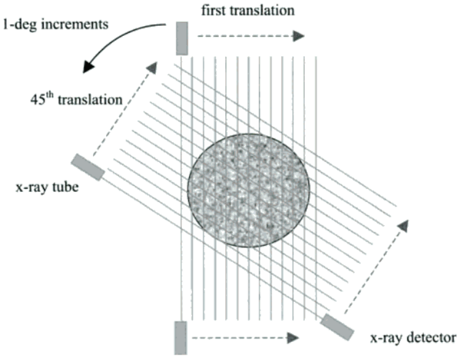

From [15], Figure 1.12

CT History

- 1895: Wilhelm Conrad Röntgen discovers X-rays
- 1963: Cormack used a collimated ^{60}Co source and a Geiger counter as a detector [12]
- 1976: Hounsfield worked on first clinical scanner [13]
- Nobel Prize in 1979, jointly for Allan Cormack and Godfrey Hounsfield
- CT scanner generations
  - First generation
  - Second generation

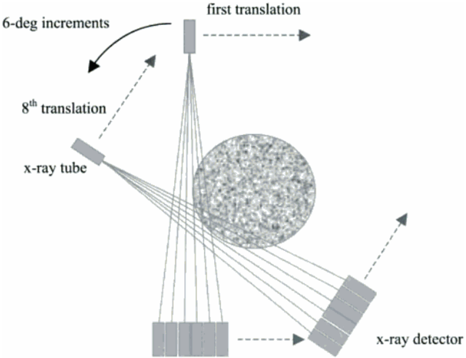

From [15], Figure 1.13

CT History

- 1895: Wilhelm Conrad Röntgen discovers X-rays
- 1963: Cormack used a collimated ^{60}Co source and a Geiger counter as a detector [12]
- 1976: Hounsfield worked on first clinical scanner [13]
- Nobel Prize in 1979, jointly for Allan Cormack and Godfrey Hounsfield
- CT scanner generations
  - First generation
  - Second generation
  - Third generation

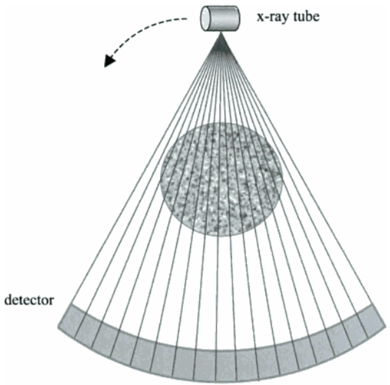

From [15], Figure 1.14

µCT History I

- X-ray computed tomography began to replace analog focal plane tomography in the early 1970s [**Lin2019**]
- Non-medical use in the late 1970s, for detection of internal defects in fabricated parts and equipment
- Lee Feldkamp [16] developed an early laboratory microCT system by assembling a micro-focus cone beam x-ray source, specimen holder and stagers, and an image intensifier at Ford Motor Company's Scientific Research Laboratory to nondestructively detect damage in ceramic manufactured automobile parts
- Feldkamp met with scientists at Henry Ford Hospital and University of Michigan interested in understanding the relationship between the microstructure and biomechanical function of trabecular bone to study osteoporotic fractures [**Feldkamp1983**]

µCT History II

- µCT was first reported in the 1980s, for scanning gemstones
- Early 1990s: Manufacturers like SkyScan and Scanco Medical made µCT systems commercially available
- Today: Nondestructive imaging for quantifying the (micro)structure of (organic) materials
  - Mineralized bone tissue and the relationships between the mechanical behavior of bone to its structural and compositional properties
  - Teeth and their internal details
  - Tissues, small animals, and medical devices like stents and implants
  - Soft tissues and vasculature using radio-opaque contrast agents
  - Characterization of anatomical details in high resolution
- $\approx$2500 µCT systems are in use worldwide with over 1000 publications annually

X-ray interaction

- “X-rays interact with tissue in 2 main ways: photoelectric effect and Compton scatter. To a first approximation, the photoelectric effect contributes to contrast while the Compton effect contributes to noise. Both contribute to dose.” ([19])
  - Photoelectric absorption (τ) is strongly dependent on the atomic number Z of the absorbing material: $\tau \propto \frac{Z^4}{E^{3.5}}$
  - Compton scattering is one of the principle forms of photon interaction and is directly proportional to the (electron & physical) density of the material. It does *not* depend on the atomic number: $\lambda' - \lambda = \frac{h}{m_e c}(1 - \cos\theta)$
- Lowering x-ray energy increases contrast
- X-ray penetration decreases exponentially with sample thickness [20, i. e. Beer-Lamberts law]: $I(t) = I_0\, e^{-\alpha z}$

Composition of biological tissues

Tissue: content by mass percentage

Element Atomic number	H 1	C 6	N 7	O 8	Na 11	P 15	S 16	Cl 17	K 19	Ca 20
Fat	11.4	59.8	0.7	27.8	0.1		0.1	0.1		
Water	11.2			88.8						
Blood	10.2	11	3.3	74.5	0.1	0.1	0.2	0.3	0.2	
Liver	10.2	13.9	3	71.6	0.3	0.2	0.3	0.2	0.3	
Brain	10.7	14.5	2.2	71.2	0.2	0.4	0.2	0.3	0.3	
Bone	3.4	15.5	4.2	43.5	0.1	10.3	0.3			22.5

Why µCT?

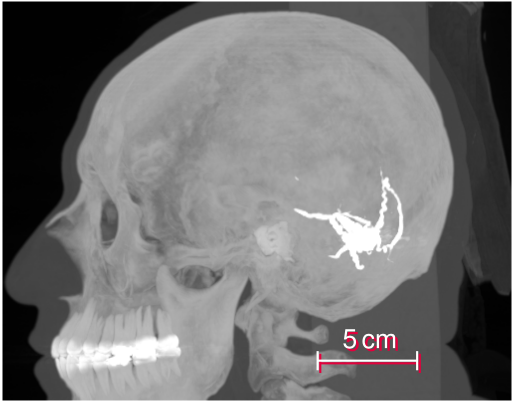

From [21], Subject *C3L-02465*

Why µCT?

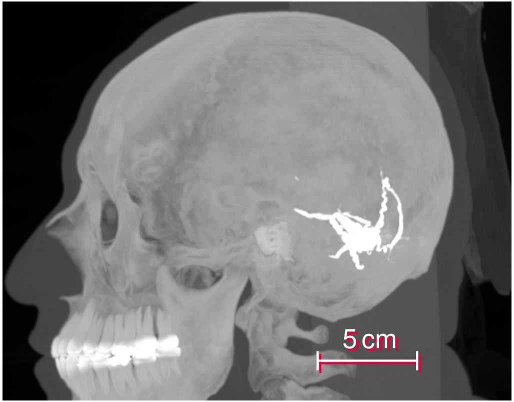

From [21], Subject *C3L-02465*

Why µCT?

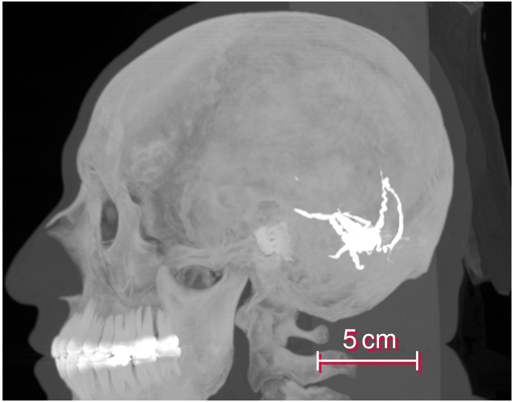

From [21], Subject *C3L-02465*

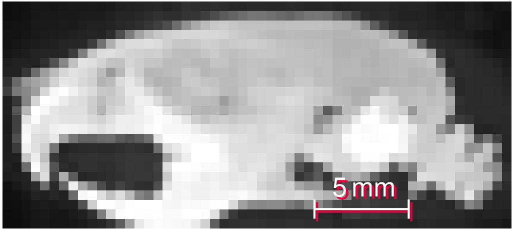

Why µCT?

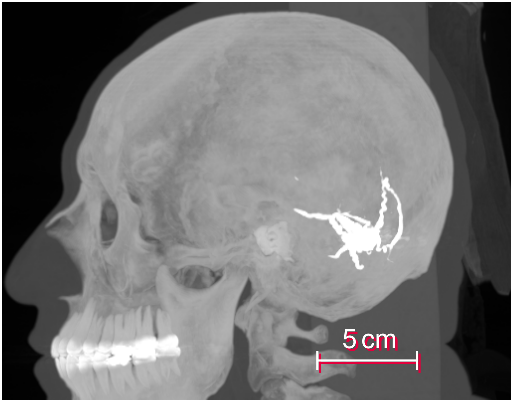

From [21], Subject *C3L-02465*

Why µCT?

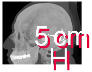

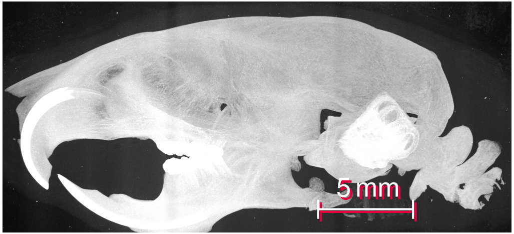

Maximum intensity projection

Projections

Reducing the dimensions of a dataset. For example projecting a volume (3D) to a surface by taking the maximum value across planes for each pixel.

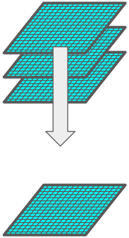

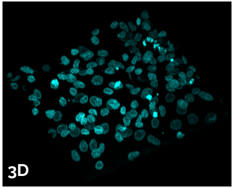

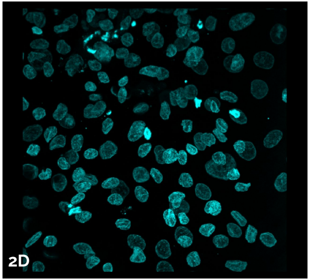

Fundamentals of Digital Image Processing by Guillaume Witz, Slide 23

Machinery

- Hospital CT
  - Voxel size around 0.5 mm
- Lab/Desktop CT
  - Voxel size around 7 µm (*in vivo*)
  - Voxel size around 0.5 µm (*ex vivo*)
- Synchrotron CT
  - Voxel size down to 160 nm

flic.kr/p/D4rbom

Machinery

- Hospital CT
  - Voxel size around 0.5 mm
- Lab/Desktop CT
  - Voxel size around 7 µm (*in vivo*)
  - Voxel size around 0.5 µm (*ex vivo*)
- Synchrotron CT
  - Voxel size down to 160 nm

Machinery

- Hospital CT
  - Voxel size around 0.5 mm
- Lab/Desktop CT
  - Voxel size around 7 µm (*in vivo*)
  - Voxel size around 0.5 µm (*ex vivo*)
- Synchrotron CT
  - Voxel size down to 160 nm

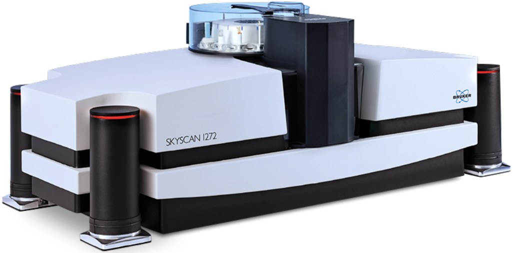

bruker.com/skyscan1272

Machinery

- Hospital CT
  - Voxel size around 0.5 mm
- Lab/Desktop CT
  - Voxel size around 7 µm (*in vivo*)
  - Voxel size around 0.5 µm (*ex vivo*)
- Synchrotron CT
  - Voxel size down to 160 nm

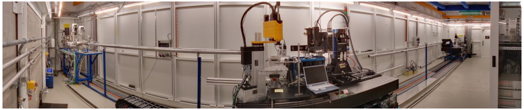

flic.kr/p/7Xhk2Y

What is happening?

No matter what kind of machine, the basic principle is always

- an x-ray source
- a sample
- a detector

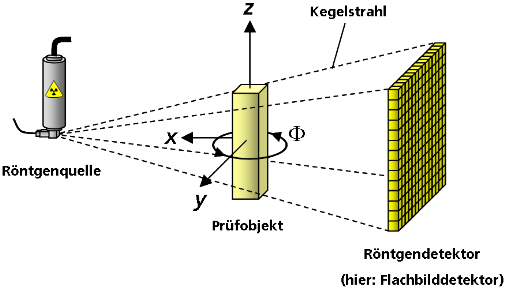

w.wiki/7g3

Machinery

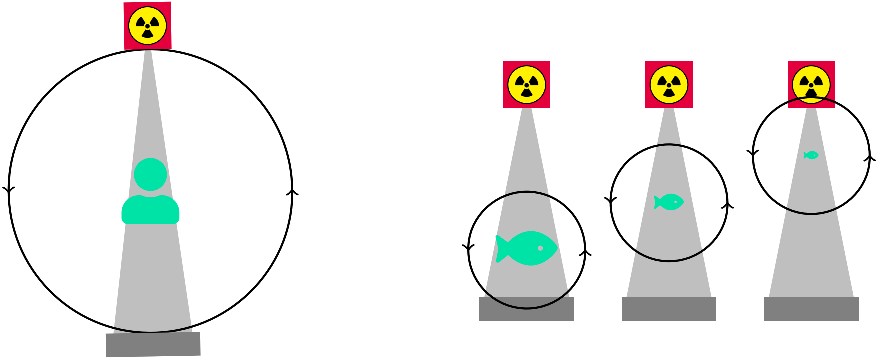

Examples

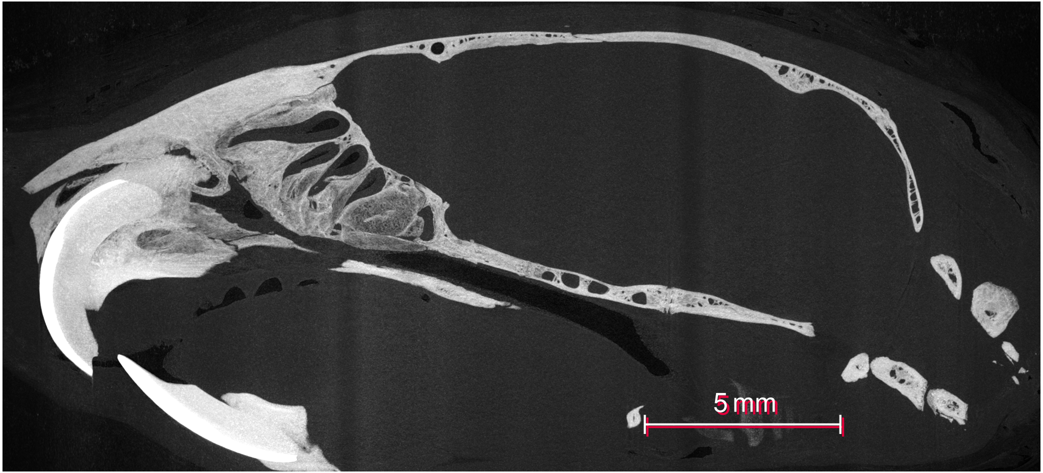

Examples

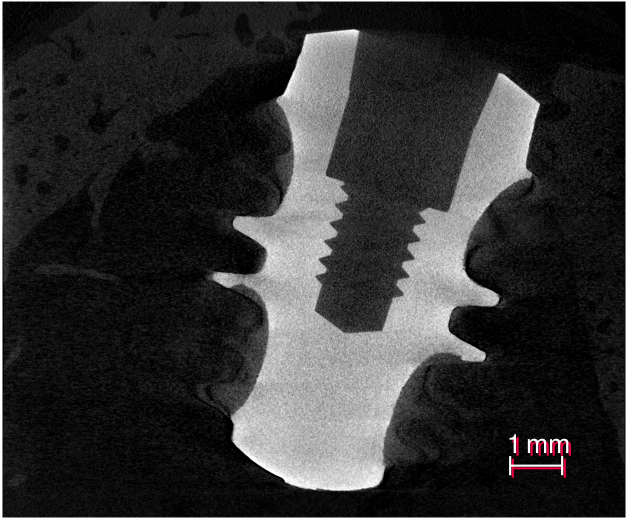

Examples

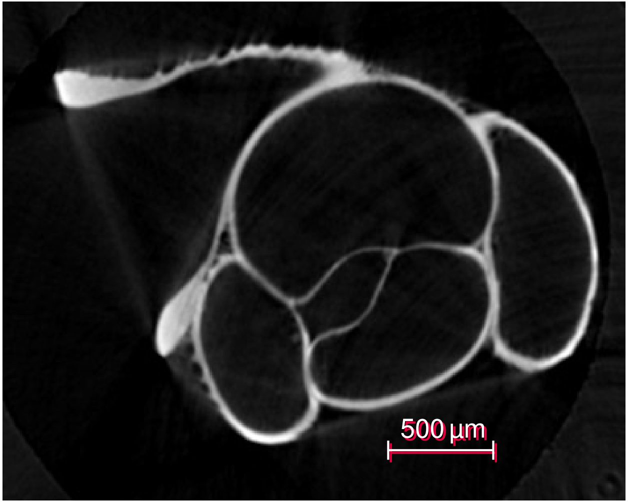

From [8], *Diancta phoenīx*

Examples

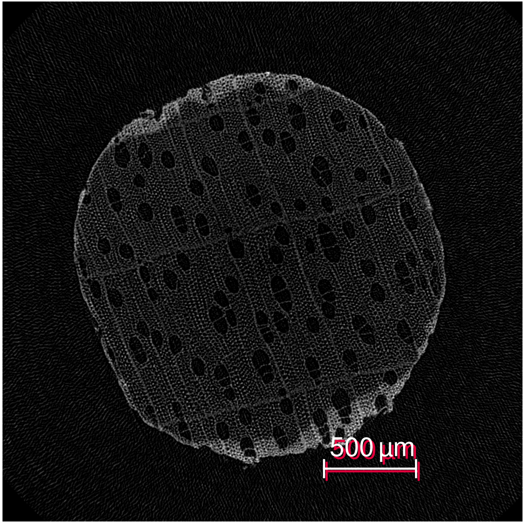

Examples

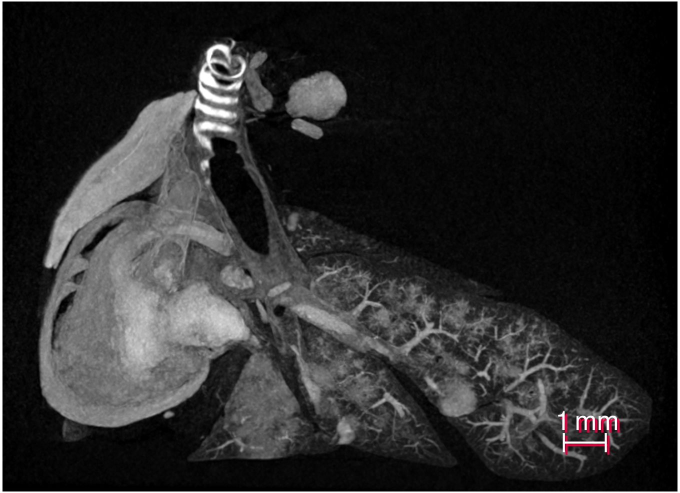

Preparation

- Study design
- Sample preparation

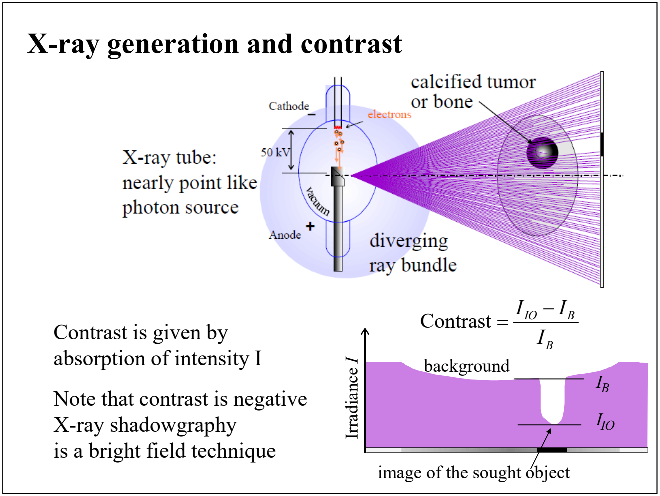

Contrast, Magnification and Resolution—Laws of Physics for Microscopists (1, 2022) by Martin Frenz, Slide 21

Projections

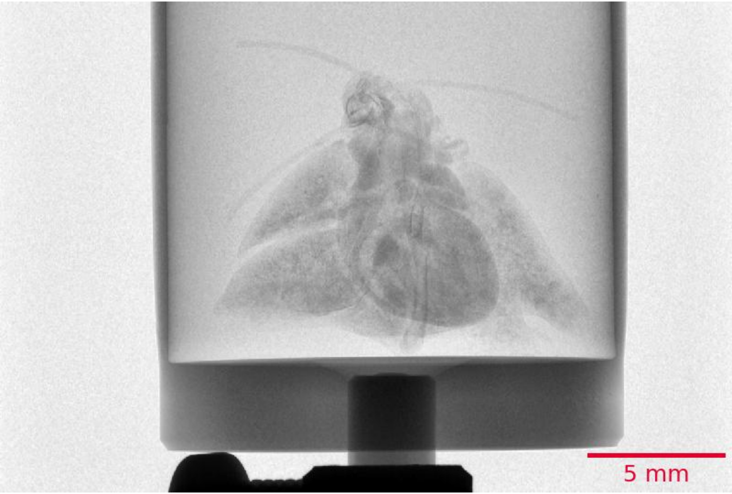

Projections

- A (micro-focus) x-ray source illuminates the object
- The x-rays penetrate the sample and are attenuated
- A scintillator converts the x-rays to visible light
- A (planar) x-ray detector collects (magnified) projection images.
- The projections are recorded on disk

Reconstructions

Reconstructions

- Based on hundreds of angular views acquired while the object rotates, a computer synthesizes a stack of virtual cross section slices through the object.
- Radon Transformation
- Filtered back projection
- Cone beam reconstruction [16]
- Corrections (beam hardening, etc.)
- Writing to stack

Visualization

Visualization

– Based on the reconstructions, a computer synthesizes a three-dimensional view of the scanned sample

Projection acquisition

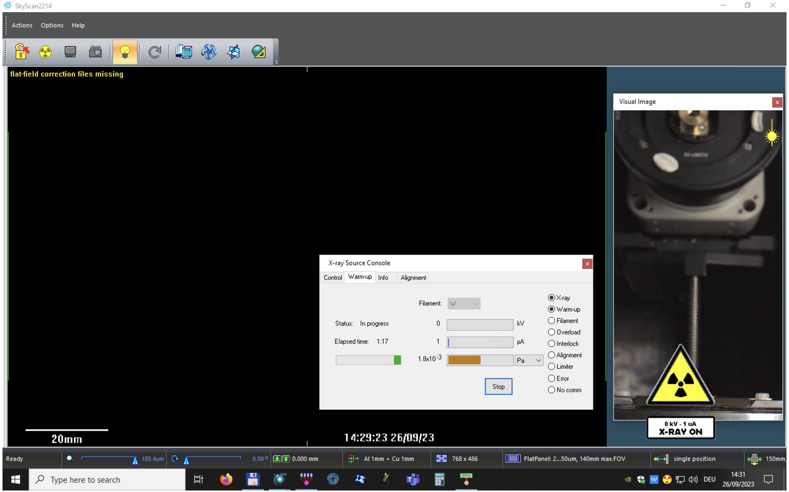

Reconstructions

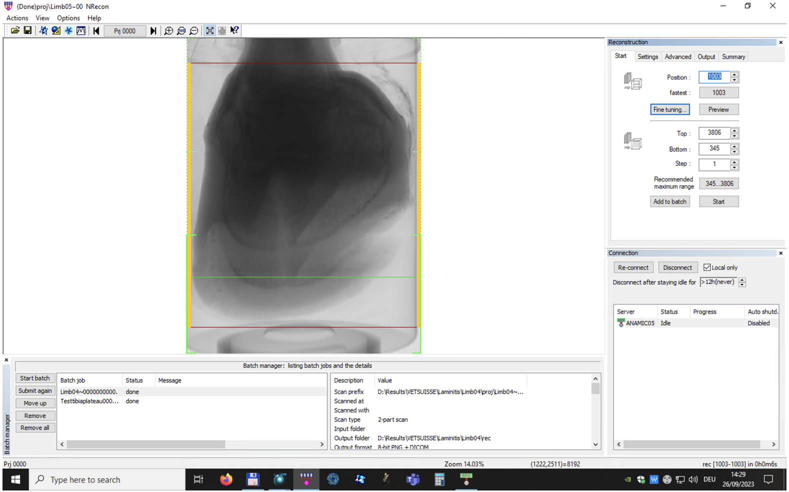

Reconstructions

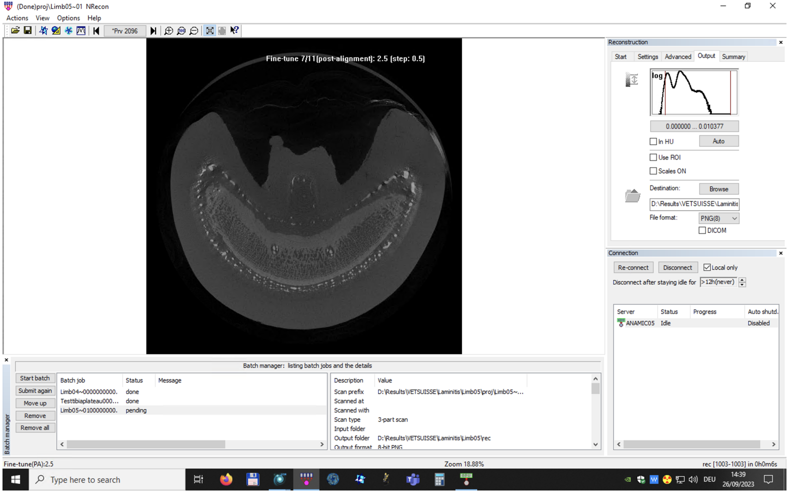

What to use?

- ImageJ/Fiji [22]
- Also see *Fundamentals of Digital Image Processing* by Guillaume Witz
- Reproducible research
  - in Jupyter [23]
  - **git**
  - Script all your things!
  - Data repositories; i. e. sharing is caring!

Quantitative data

- Pretty images are nice to have, but science is built on quantitative data.
- Segmentation
- Characterization

Internal morphology of human teeth

Collaboration with zmk bern Zahnmedizinische Kliniken

- Num
- S

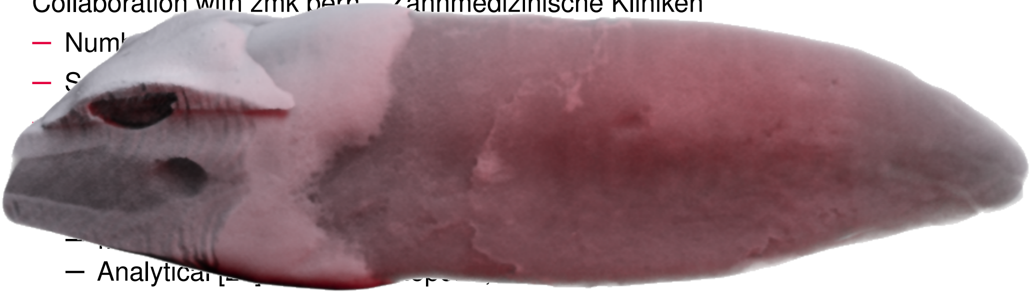

  - Analytical [

How?

- 104 extracted human permanent mandibular canines
- µCT imaging
- Root canal configuration, according to Briseño-Marroquín et al. [25]
- *Reproducible* analysis [26], e. g. you can click a button to double-check or recalculate the results yourself!

How?

- 104 extracted human permanent mandibular canines
- µCT imaging
- Root canal configuration, according to Briseño-Marroquín et al. [25]
- *Reproducible* analysis [26], e. g. you can click a button to double-check or recalculate the results yourself!

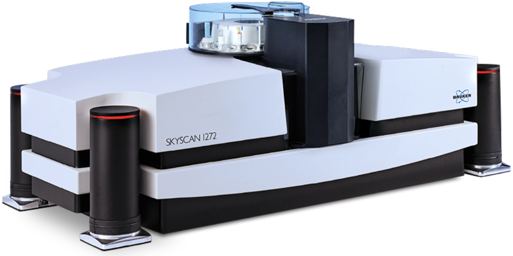

bruker.com/skyscan1272

How?

- 104 extracted human permanent mandibular canines
- µCT imaging
- Root canal configuration, according to Briseño-Marroquín et al. [25]
- *Reproducible* analysis [26], e. g. you can click a button to double-check or recalculate the results yourself!

```
Scanner=SkyScan1272
Instrument S/N=15G09089-B
Software Version=1.1.19
Filename Prefix=Tooth045~00
Number Of Files=  482
Number Of Rows= 1092
Number Of Columns= 1632
Source Voltage (kV)=  80
Source Current (uA)= 125
Image Pixel Size (um)=9.999986
Exposure (ms)=950
Rotation Step (deg)=0.400
Frame Averaging=ON (3)
Filter=Al 1mm
Study Date and Time=02 Jul 2020  08h:23m:34
    s
Scan duration=0h:39m:51s
```

How?

- 104 extracted human permanent mandibular canines
- µCT imaging
- Root canal configuration, according to Briseño-Marroquín et al. [25]
- *Reproducible* analysis [26], e. g. you can click a button to double-check or recalculate the results yourself!

Sample changer on the SkyScan 1272
In total:

- 13 days of *continuous* µCT scanning
- 819 GB of raw data
  230 648 TIFF projections
- 326 GB data as input for analysis
  282 062 PNG reconstructions

How?

- 104 extracted human permanent mandibular canines
- µCT imaging
- Root canal configuration, according to Briseño-Marroquín et al. [25]
- *Reproducible* analysis [26], e. g. you can click a button to double-check or recalculate the results yourself!

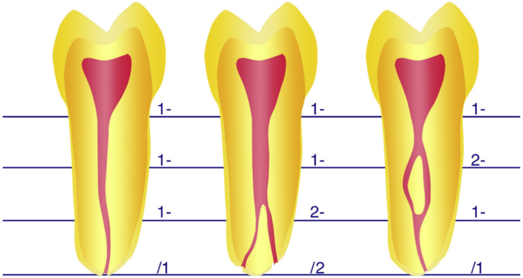

From [25], Fig. 2

How?

- 104 extracted human permanent mandibular canines
- µCT imaging
- Root canal configuration, according to Briseño-Marroquín et al. [25]
- *Reproducible* analysis [26], e. g. you can click a button to double-check or recalculate the results yourself!

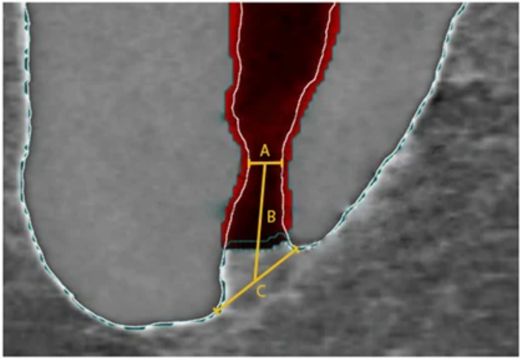

From [27], Fig. 1

How?

- 104 extracted human permanent mandibular canines
- µCT imaging
- Root canal configuration, according to Briseño-Marroquín et al. [25]
- *Reproducible* analysis [26], e. g. you can click a button to double-check or recalculate the results yourself!

gph.is/2nqkple

How?

- 104 extracted human permanent mandibular canines
- µCT imaging
- Root canal configuration, according to Briseño-Marroquín et al. [25]
- *Reproducible* analysis [26], e. g. you can click a button to double-check or recalculate the results yourself!

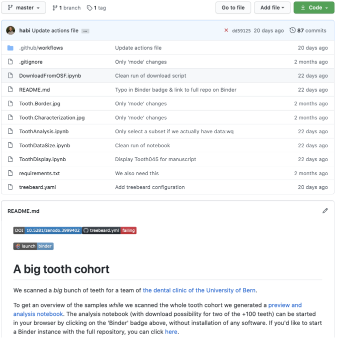

µCT imaging

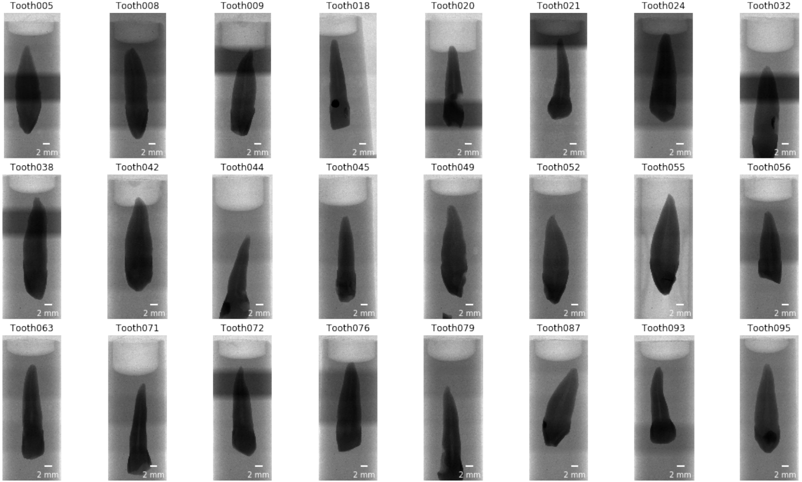
Tooth005
Tooth008
Tooth009
Tooth018
Tooth020
Tooth021
Tooth024
Tooth032
Tooth038
Tooth042
Tooth044
Tooth045
Tooth049
Tooth052
Tooth055
Tooth056
Tooth063
Tooth071
Tooth072
Tooth076
Tooth079
Tooth087
Tooth093
Tooth095
2 mm

Dataset cropping

- Full datasets: 326 GB
- Cropped datasets: 115 GB

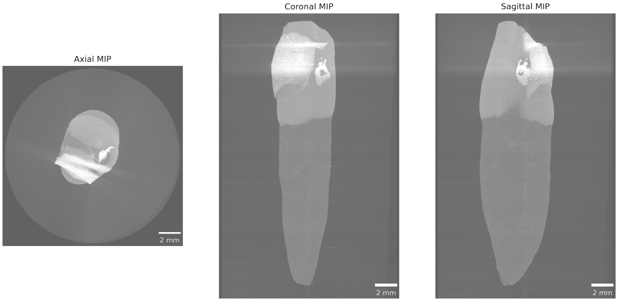

Dataset cropping

- Full datasets: 326 GB
- Cropped datasets: 115 GB

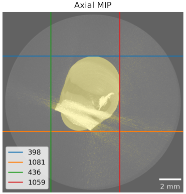

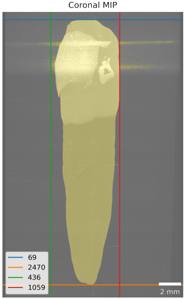

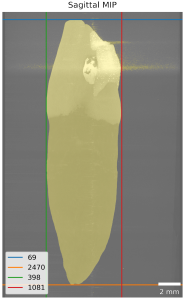

Tooth morphology

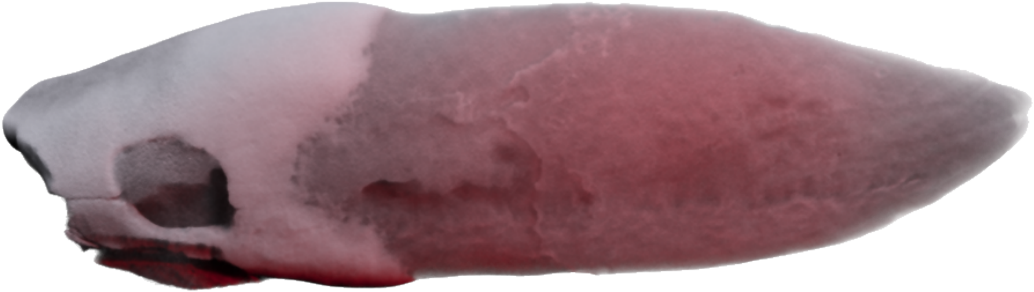

Tooth morphology

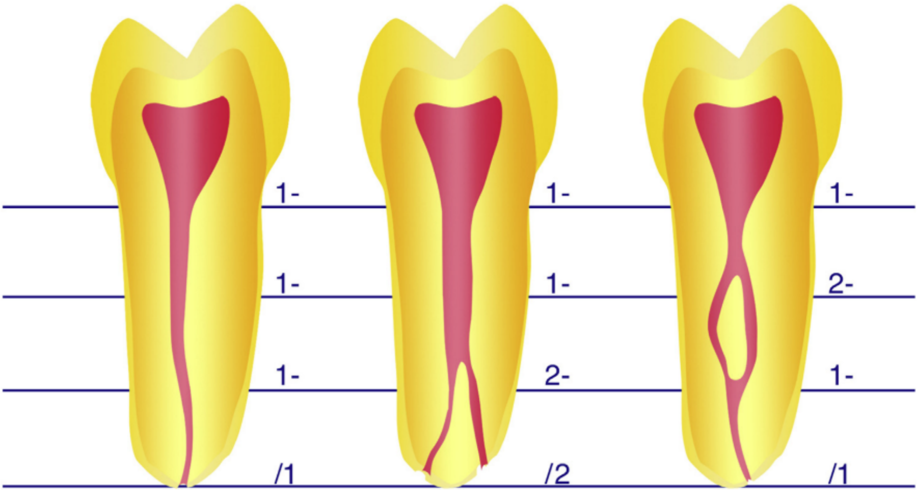

From [25], Fig. 2

Tooth morphology

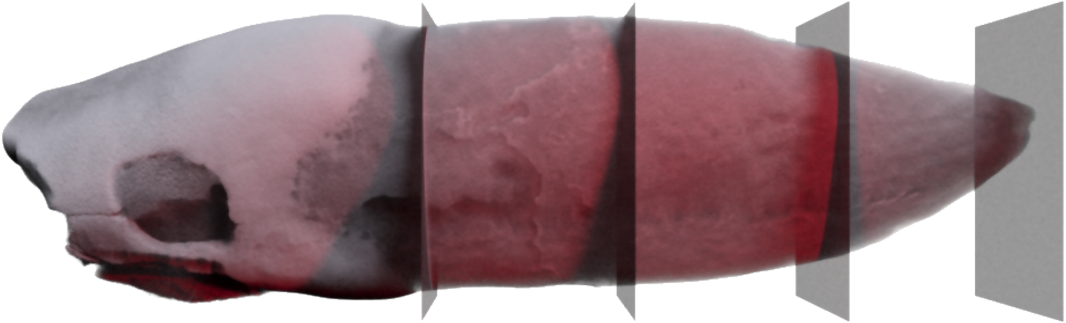

Detection of enamel-dentin border

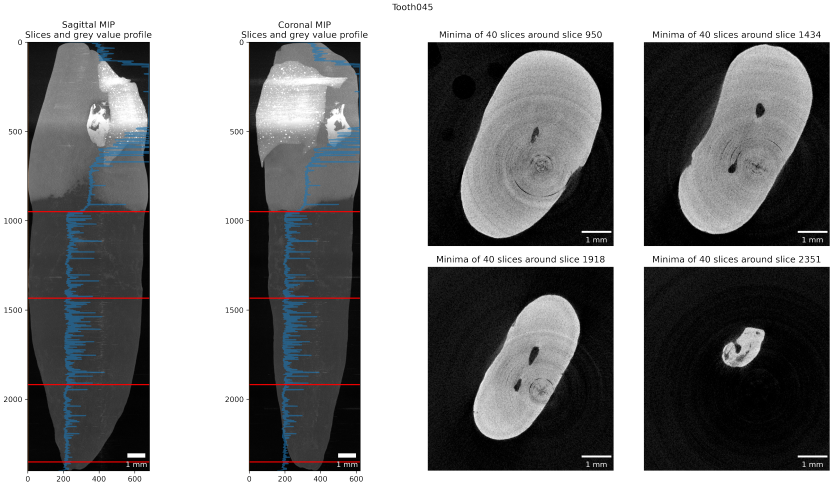

Detection of enamel-dentin border

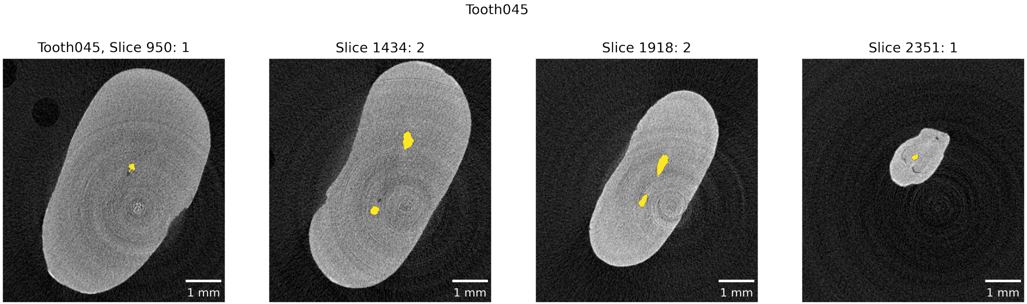

Classification of root canal configurations

Roots		RCC	#	%
Single (N=98)		1-1-1/1	73	74.5
		1-1-1/2	14	14.3
		1-1-1/3	1	1.0
		1-1-1/4	2	2.1
		1-1-2/1	1	1.0
		1-2-1/1	4	4.1
		1-2-1/2	1	1.0
		1-2-2/2	1	1.0
		2-3-1/1	1	1.0
Double (N=3)	Buccal	1-1-1/1	2	66.6
		1-2-1/1	1	33.3
	Lingual	1-1-1/1	2	66.6
		1-1-1/2	1	33.3

Extraction of root canal space

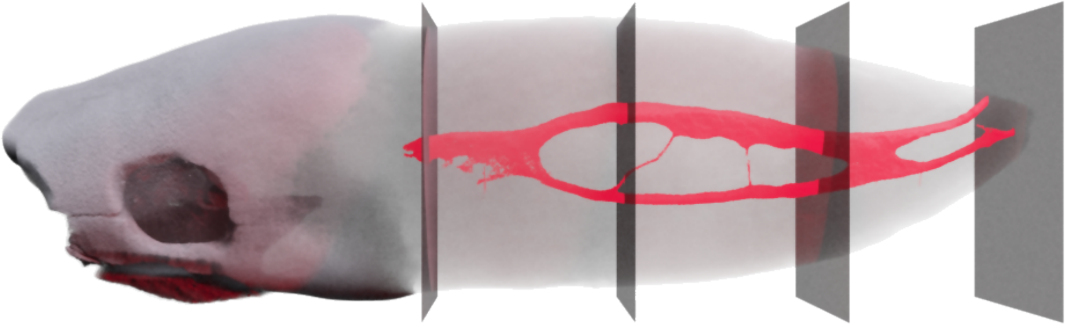

Results of root canal space extraction

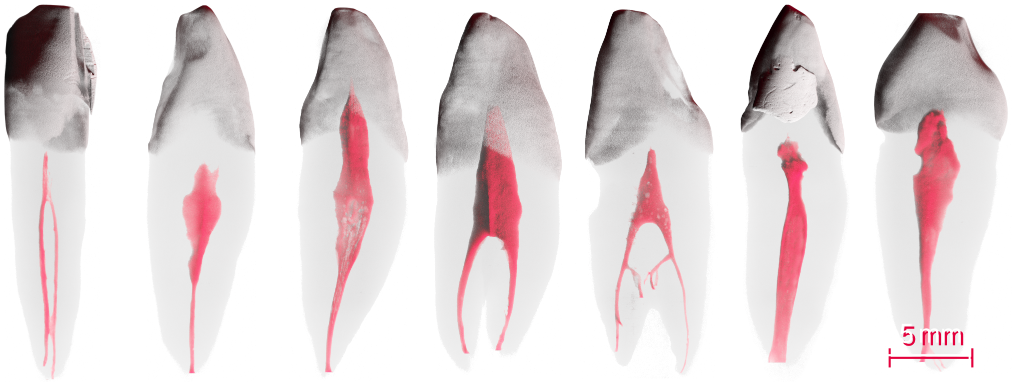

Physiological foramen geometry

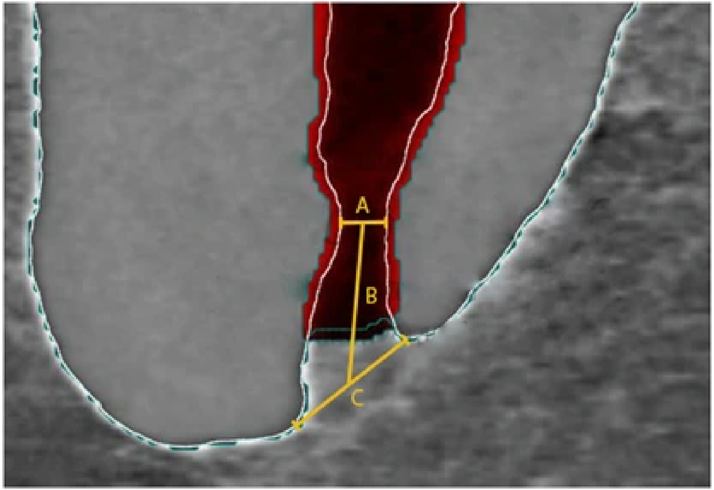

From [27], Fig. 1

Physiological foramen geometry

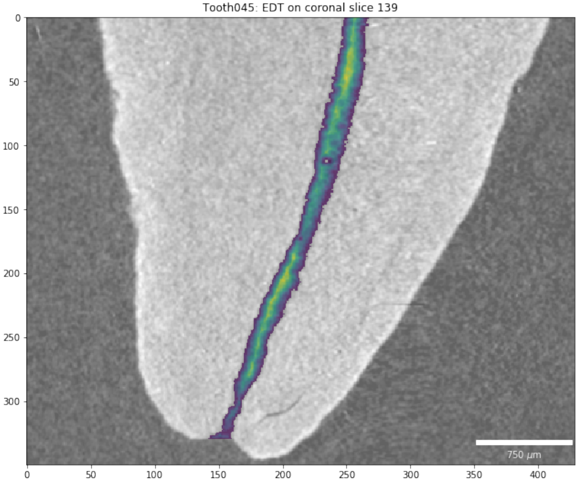

Conclusion ZMK

- Efficient use of time, e. g. more teeth does not mean more (human) work
- Reproducible analysis with *free and open-source* software, usable by *anyone*
- Objective analysis, e. g. no operator bias

Metal foam

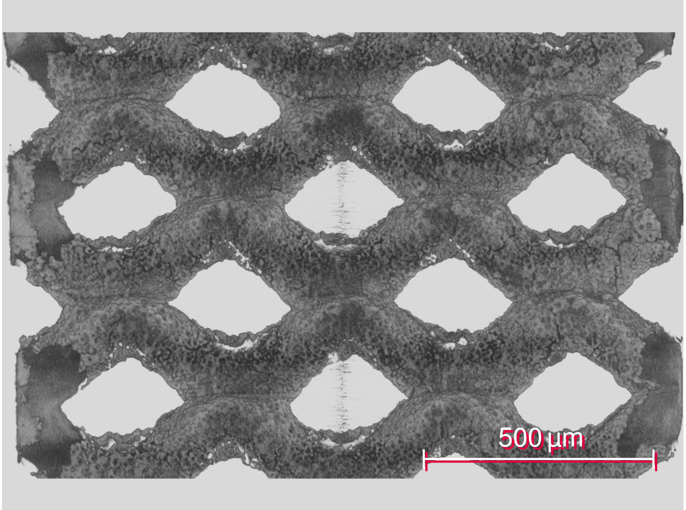

Etienne Berner NanoElectroCatalysis Group

Data wrangling by example: Cichlids

Collaboration with the Institute of Ecology and Evolution [11]

- 133 Cichlids from Lake Victoria, East Africa
  - Functional anatomy of the skulls and jaws
  - 6–18 cm in size
- 375 scans in total
  - Voxelsizes from 3.5–50 µm
  - 46 days of scanning time
  - 9.8 TB of raw data
  - 1.5 TB/+1 000 000 reconstructions

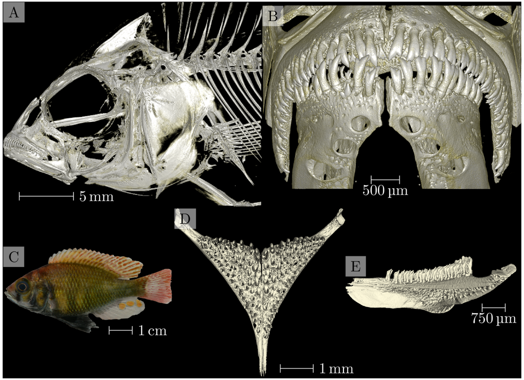

DOI:gsst8t, Fig. 1

Visualization of cichlid head

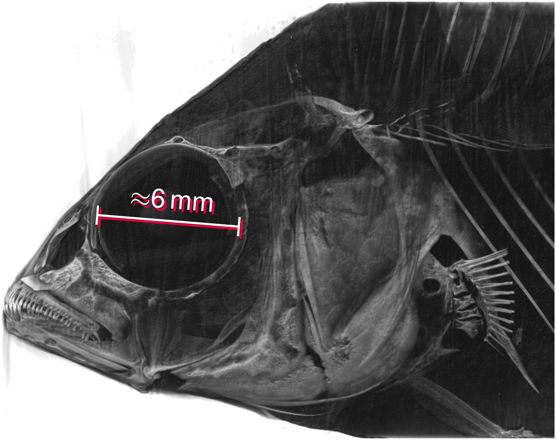

Visualization of cichlid head

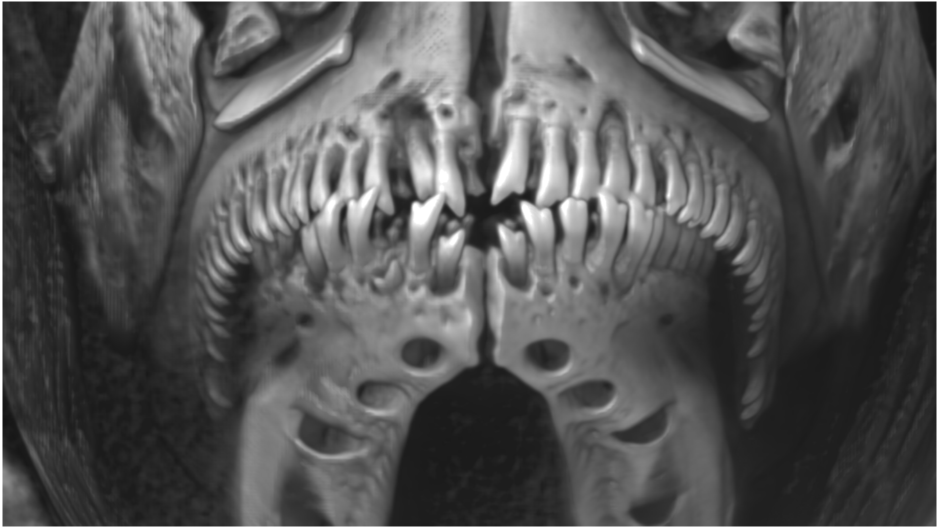

Visualization of segmented pharyngeal jaw

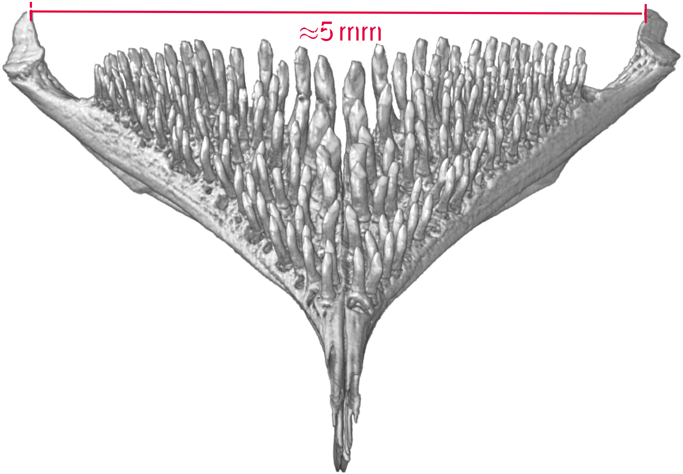

Data wrangling by example: Cichlids

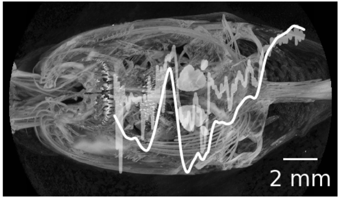

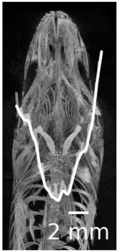

Data wrangling by example: Cichlids

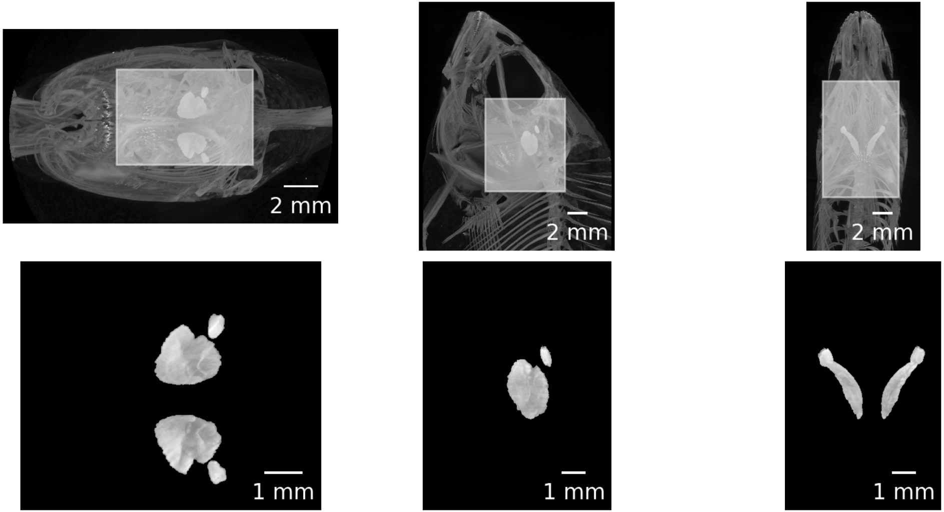

Thanks!

- Thanks for listening to me!
- What questions do you have for me?

References I

[1] Ruslan Hlushchuk et al. “Cutting-Edge Microangio-CT: New Dimensions in Vascular Imaging and Kidney Morphometry”. (Mar. 2018). DOI: 10.1152/ajprenal.00099.2017 (slide 5).

[2] Henry Nording et al. “The C5a/C5a Receptor 1 Axis Controls Tissue Neovascularization through CXCL4 Release from Platelets”. (Dec. 2021). DOI: 10.1038/s41467-021-23499-w (slide 5).

[3] Ruslan Hlushchuk et al. “Innovative High-Resolution microCT Imaging of Animal Brain Vasculature”. (Oct. 2020). DOI: 10.1007/s00429-020-02158-8 (slide 5).

[4] Tsering Wüthrich et al. “Development of Vascularized Nerve Scaffold Using Perfusion-Decellularization and Recellularization”. (Aug. 2020). DOI: 10.1016/j.msec.2020.111311 (slide 5).

[5] Cédric Zubler et al. “The Anatomical Reliability of the Superficial Circumflex Iliac Artery Perforator (SCIP) Flap”. (Mar. 2021). DOI: 10.1016/j.aanat.2020.151624 (slide 5).

References II

[6] Matthias Messerli et al. “Adaptation Mechanism of the Adult Zebrafish Respiratory Organ to Endurance Training”. (Feb. 2020). DOI: 10.1371/journal.pone.0228333 (slide 5).

[7] Verdiana Trappetti et al. “Synchrotron Microbeam Radiotherapy for the Treatment of Lung Carcinoma: A Pre-Clinical Study”. (Aug. 2021). DOI: 10.1016/j.ijrobp.2021.07.1717 (slide 5).

[8] Estée Bochud et al. “A New Diancta Species of the Family Diplommatinidae (Cyclophoroidea) from Vanua Levu Island, Fiji”. (Nov. 2021). DOI: 10.3897/zookeys.1073.73241 (slide 5, 38).

[9] Sebastian Halm et al. “Micro-CT Imaging of Thiel-embalmed and Iodine-Stained Human Temporal Bone for 3D Modeling”. (2021). DOI: 10.1186/s40463-021-00522-0 (slide 5).

[10] David Haberthür et al. “Automated Segmentation and Description of the Internal Morphology of Human Permanent Teeth by Means of Micro-CT”. (Apr. 2021). DOI: gjpw2d (slide 5, 54).

References III

[11] David Haberthür et al. “Microtomographic Investigation of a Large Corpus of Cichlids”. (Sept. 2023). DOI: gsst8t (slide 5, 78).

[12] A. M. Cormack. “Representation of a Function by Its Line Integrals, with Some Radiological Applications”. (Sept. 1963). DOI: 10.1063/1.1729798 (slide 14).

[13] Godfrey Newbold Hounsfield. “Historical Notes on Computerized Axial Tomography.”. (1976) (slide 14).

[14] E C Beckmann. “CT Scanning the Early Days.”. (Jan. 2006). DOI: 10.1259/bjr/29444122 (slide 15).

[15] J Hsieh. *Computed Tomography: Principles, Design, Artifacts, and Recent Advances*. Society of Photo Optical, 2003 (slide 17, 18, 19).

[16] L. A. Feldkamp et al. “Practical Cone-Beam Algorithm”. (June 1984). DOI: 10.1364/JOSAA.1.000612 (slide 20, 46).

[17] L. A. Feldkamp et al. “The Direct Examination of Three-Dimensional Bone Architecture in Vitro by Computed Tomography”. (Feb. 1989). DOI: 10.1002/jbmr.5650040103.

References IV

[18] M. W. Layton et al. "Examination of Subchondral Bone Architecture in Experimental Osteoarthritis by Microscopic Computed Axial Tomography". (Nov. 1988). DOI: 10.1002/art.1780311109.

[19] Mark Hammer. *X-Ray Physics: X-Ray Interaction with Matter, X-Ray Contrast, and Dose*. (Slide 22).

[20] Wikipedia contributors. *Beer–Lambert Law — Wikipedia, The Free Encyclopedia*. 2019 (slide 22).

[21] Kenneth Clark et al. "The Cancer Imaging Archive (TCIA): Maintaining and Operating a Public Information Repository". (Dec. 2013). DOI: 10.1007/s10278-013-9622-7 (slide 24).

[22] Johannes Schindelin et al. "Fiji: An Open-Source Platform for Biological-Image Analysis". (July 2012). DOI: 10.1038/nmeth.2019 (slide 52).

[23] Thomas Kluyver et al. "Jupyter Notebooks – a Publishing Format for Reproducible Computational Workflows". (2016). DOI: 10.3233/978-1-61499-649-1-87 (slide 52, 54).

References V

[24] Thomas Gerhard Wolf et al. “Internal Morphology of 101 Mandibular Canines of a Swiss-German Population by Means of Micro-CT: An Ex Vivo Study”. (2021). DOI: g7r8 (slide 54).

[25] Benjamín Briseño-Marroquín et al. “Root Canal Morphology and Configuration of 179 Maxillary First Molars by Means of Micro–Computed Tomography: An Ex Vivo Study”. (Dec. 2015). DOI: 10.1016/j.joen.2015.09.007 (slide 55).

[26] David Haberthür. “Habi/Zmk-Tooth-Cohort: Used for Manuscript about Method”. (Aug. 2020). DOI: 10.5281/ZENODO.3999402 (slide 55).

[27] Thomas Gerhard Wolf et al. “Three-Dimensional Analysis of the Physiological Foramen Geometry of Maxillary and Mandibular Molars by Means of Micro-CT”. (Sept. 2017). DOI: 10.1038/ijos.2017.29 (slide 60, 74).

Colophon

- This BEAMER presentation was crafted in LaTeX with the (slightly adapted) template from *Corporate Design und Vorlagen* of the University of Bern.
  - Complete source code: git.io/fjpP7
  - The LaTeX code is automatically compiled with a GitHub action to a (handout) PDF which you can access here: git.io/JeQxO
- Did you spot an error?
  - File an issue: git.io/fjpPb
  - Submit a pull request: git.io/fjpPN
  - Send me an email: david.haberthuer@unibe.ch